



Distinct vitellogenin domains differentially regulate immunological outcomes in invertebrates

Received for publication, August 20, 2020, and in revised form, November 5, 2020. Published, Papers in Press, November 11, 2020.
<https://doi.org/10.1074/jbc.RA120.015686>

Weikang Sun[‡], Hao Li[‡], Yuehong Zhao, Longwei Bai, Yukai Qin, Qun Wang[Ⓜ], and Weiwei Li^{*Ⓜ}

From the Laboratory of Invertebrate Immunological Defense and Reproductive Biology, School of Life Sciences, East China Normal University, Shanghai, China

Edited by Chris Whitfield

The classical role of Vitellogenin (Vg) is providing energy reserves for developing embryos, but its roles appear to extend beyond this nutritional function, and its importance in host immune defense is garnering increasing research attention. However, Vg-regulated immunological functions are dependent on three different domains within different species and remain poorly understood. In the present study, we confirmed three conserved VG domains—LPD_N, DUF1943, and VWD—in the Chinese mitten crab (*Eriocheir sinensis*), highlighting functional similarities of Vg in vertebrates and invertebrates. Of these three domains, DUF1943 and VWD showed definitive bacterial binding activity *via* interaction with the signature components on microbial surfaces, but this activity was not exhibited by the LPD_N domain. Antibacterial assays indicated that only the VWD domain inhibits bacterial proliferation, and this function may be conserved between different species due to the conserved amino acid residues. To further explore the relationship between Vg and polymeric immunoglobulin receptor (pIgR), we expressed *Esp*IgR and the three *E. sinensis* Vg (*Es*Vg) domains in HEK293T cells, and coimmunoprecipitation assay demonstrated that only the DUF1943 domain interacts with *Esp*IgR. Subsequent experiments demonstrated that *Es*Vg regulates hemocyte phagocytosis by binding with *Esp*IgR through the DUF1943 domain, thus promoting bacterial clearance and protecting the host from bacterial infection. To the best of our knowledge, our work is the first to report distinct domains in Vg inducing different immunological outcomes in invertebrates, providing new evidence that pIgR acts as a phagocytic receptor for Vg.

Vitellogenin (Vg) is a member of the large lipid transfer protein (LLTP) superfamily, which also includes the microsomal triglyceride transfer protein and apolipoprotein (1, 2). As an egg yolk precursor protein, Vg is present in the females of nearly all oviparous species, including fish, amphibians, reptiles, birds, most invertebrates, and the platypus (3). Vg is usually synthesized extra-ovarianly and then transported by the circulation system to the ovaries, where it is internalized

into growing oocytes *via* receptor-mediated endocytosis and then proteolytically cleaved to generate the yolk proteins lipovitellin (Lv) and phosvitin (Pv), providing nutrients to developing embryos (4). However, there is an increasing body of evidence indicating that its roles extend beyond this nutritional function, and its role in host immune defense is attracting considerable research attention (5).

For instance, recent studies have shown that Vg in vertebrate plays a role in its immune response, either as a pattern recognition molecule that recognizes bacteria or as an opsonin to enhance macrophage phagocytosis (6, 7). Furthermore, Vg has been reported to directly kill bacteria *via* interactions with lipopolysaccharides and lipoteichoic acid present in bacterial cell walls and to neutralize viruses by binding to and creating cross-links between virions (8). Several studies on the immunological functions of Vg in invertebrate have also been reported. For example, Vg in the mosquito *Anopheles gambiae* is able to interfere with antiplasmodium response by reducing the parasite-killing efficiency of the antiparasitic factor TEP1 (9). Vg in honeybees also has immunological binding properties and is able to mediate previous unexpected trans-generational immunity by transporting microbe-derived molecules into developing eggs (10, 11).

Vg is a high-molecular-mass glycolipophosphoprotein that typically circulates in the blood/hemolymph as a homodimer. It is encoded by multiple genes in several species including insects, fish, and frogs (12). Vg is considered to have similar characteristics in vertebrates, such as fish, and invertebrates, particularly crustacea (5). Typically, Vg contains three conserved domains: LPD_N (*i.e.*, vitellogenin N or LLT), which has been identified in the N-terminus of LLTP members; DUF1943, the function of which is unclear; and the von Willebrand factor type D domain (VWD), which is located at the C-terminus and distributed over a wide range of proteins (13). The N-terminal LPD_N domain encodes the Lv heavy chain (LvH), whereas the C-terminal VWD encodes the β -component (5).

Scanning electron microscopy as well as bacterial cell and protoplast lysis assay studies of fish have shown that Vg is able to lyse both *Escherichia coli* and *Staphylococcus aureus*, and the coating *E. coli*, *S. aureus*, and *P. pastoris* with Vg facilitates the phagocytosis of these microbes by macrophages (7), indicating that Vg is an opsonin, *i.e.*, a bridging molecule between

This article contains supporting information.

[‡] These authors contributed equally to this work.

* For correspondence: Weiwei Li, wwli@bio.ecnu.edu.cn.

Vitellogenin regulates phagocytosis in crab

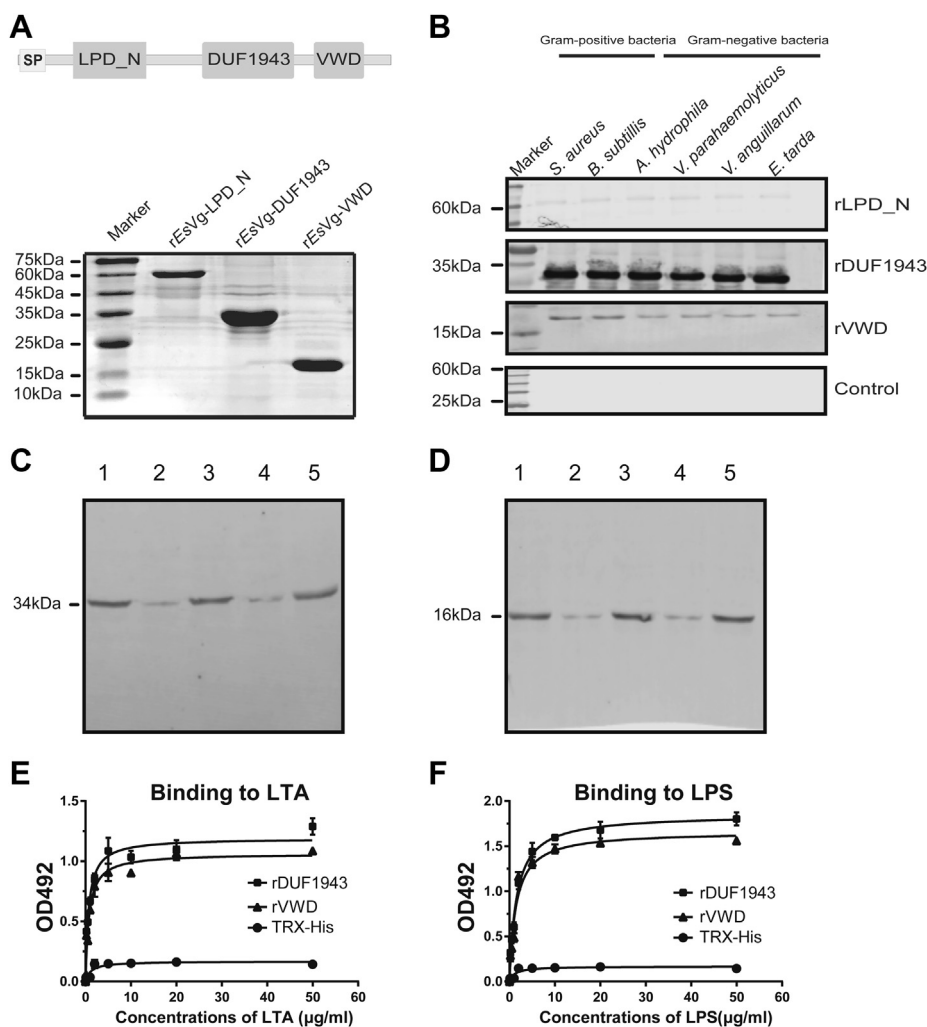


Figure 1. *EsVg* binds to bacteria through different domains. *A*, expression of different *rEsVg* domains in truncated proteins. Proteins were expressed in *E. coli* and then purified by affinity chromatography with Ni-NTA beads. *Top panel*, schematic illustration of the partial expression of *EsVg*; *Bottom panel*, SDS-PAGE of the purified proteins. *B*, binding properties of *EsVg* to bacteria. Western blotting was performed to analyze six bacterial strains incubated with *rEsVg*-LPD_N, *rEsVg*-DUF1943, and *rEsVg*-VWD (rLPD_N, rDUF1943, rVWD). Following three washes with PBS, bacterial cell pellets and the supernatant from the final PBS wash (control) were analyzed. The bacterial strains are *Staphylococcus aureus*, *Bacillus subtilis*, *Aeromonas hydrophila*, *Vibrio Parahaemolyticus*, *Vibrio anguillarum*, and *Edwardsiella tarda*. *C–F*, binding of rDUF1943 and rVWD to LTA and LPS. Binding of rDUF1943 (*C*) and rVWD (*D*) to *S. aureus* and *V. Parahaemolyticus* was inhibited by the presence of LTA and LPS respectively. Lane 1, purified recombinant proteins; lane 2, *S. aureus* incubated with recombinant proteins, which were preincubated with LTA; lane 3, *S. aureus* incubated with recombinant proteins, which were preincubated with PBS; lane 4, *V. Parahaemolyticus* incubated with recombinant proteins, which were preincubated with LPS; lane 5, *V. Parahaemolyticus* incubated with recombinant proteins, which were preincubated with PBS. Quantitative binding of rDUF1943 and rVWD to LTA (*E*) and LPS (*F*) was analyzed by ELISA. TRX-His-tag peptide was used as control. Data are representative of at least three independent experiments.

microbes and macrophages. However, whether this function of Vg is conserved within invertebrates still remains to be demonstrated. Furthermore, the possible bacterial binding and phagocytosis-promoting functions mediated by the LPD_N, DUF1943, and VWD domains are still largely unknown, for both vertebrates and invertebrates, as is the phagocytic receptor that binds and regulates Vg-promoted bacterial phagocytosis.

Results

EsVg binds to bacteria and exerts antibacterial activity via different domains

Vg is widely considered to have the ability to bind bacteria (6, 7). However, the specific domains where Vg binds to bacteria

are still very unclear in both vertebrates and invertebrates. To investigate whether *EsVg* binds to different kinds of bacteria and to identify which domain performs the function of binding bacteria, recombinant proteins of different *EsVg* domains, *i.e.*, *rEsVg*-LPD_N, *rEsVg*-DUF1943, and *rEsVg*-VWD, were expressed in *E. coli* (Fig. 1A). The proteins were used in bacteria-binding assays to determine their ability to bind bacteria. Six different kinds of Gram-positive and Gram-negative bacteria were fully coated by *rEsVg*. Interestingly, as shown in Figure 1B, the DUF1943 domain has a strong bacteria-binding ability for Gram-positive and Gram-negative bacteria. Furthermore, the VWD domain has a comparative weak bacteria-binding ability for Gram-positive and Gram-negative bacteria. However, the results clearly show that the LPD_N domain of *EsVg* has no bacteria-binding ability.

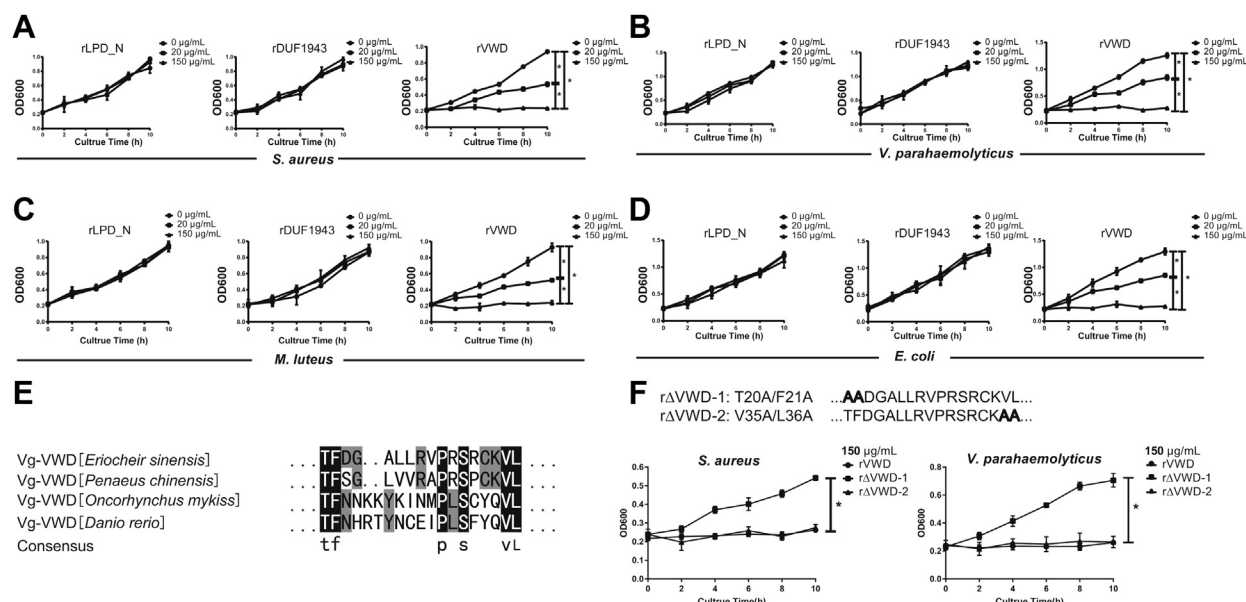


Figure 2. Growth suppression effect of the varied domain of EsVg against different bacteria. A–D, growth suppression effect of the LPD_N, DUF1943, and VWD domain of EsVg against *S. aureus* (A), *V. parahaemolyticus* (B), *M. luteus* (C), and *E. coli* (D). Bacteria were washed and suspended in the same volume of TBS with 0 µg/ml, 20 µg/ml or 150 µg/ml EsVg. E, sequence alignment between VWD from four species showed comparative similar regions from *E. sinensis* T20 to L36. F, mutated *E. sinensis* rVWD with indicated point mutants that displayed in bold and named rΔVWD-1 and rΔVWD-2, respectively (upper panel), growth suppression effect of the rΔVWD-1 and rΔVWD-2 of EsVg against *S. aureus* and *V. parahaemolyticus* (lower panel). The OD600 was measured every 2 h to obtain a growth curve of the different samples. TBS was used as the control. Data are means ± SD of triplicate experiments. Statistical significance was determined by one-way analysis of variance and post-hoc Duncan’s multiple range tests. **p* < 0.05.

To better understanding the microbial-binding activity of EsVg, Western blotting and ELISA were employed to study the effects of LTA and LPS in Gram-positive and Gram-negative bacteria on the binding of rDUF1943 and rVWD to microbes. Results have shown that the binding of rDUF1943 and rVWD to *S. aureus* and *Vibrio parahaemolyticus* was inhibited by LTA and LPS, respectively (Fig. 1, C–D), which indicated that these domains bound to the Gram-positive and Gram-negative bacteria via interaction with the signature components on microbial surfaces. ELISA was performed to verify the possible interaction between rDUF1943 and rVWD with LTA and LPS. Results have shown that both rDUF1943 and rVWD protein had a significantly stronger (*p* < 0.05) affinity to the LTA (Fig. 1E) and LPS (Fig. 1F), which demonstrated that DUF1943 and VWD domain in EsVg may specifically recognize Gram-positive and Gram-negative bacteria via LTA and LPS, respectively.

Bacteria growth inhibition of EsVg

Considering the possible role of EsVg in innate immune defense and binding bacteria (14–17), we investigated whether these domains of EsVg inhibited the growth of bacteria. The inhibitory effects of the rLPD_N, rDUF1943, and rVWD of EsVg on the growth of *S. aureus* (Fig. 2A), *Vibrio parahaemolyticus* (Fig. 2B), *M. luteus* (Fig. 2C), and *E. coli* (Fig. 2D) were analyzed. Results have shown that bacteria growth was not inhibited by 0 mg/ml of each recombinant protein, and only rVWD could significantly inhibit the growth of different bacteria in a dose-dependent manner, rather than rLPD_N and rDUF1943. Collective results suggest the unique role of VWD

domain in bacteria growth inhibition while the LPD_N and DUF1943 domains may participate in other immune responses. To understanding the function of conserved amino acid residues among VWD domain from different species on bacterial growth inhibition, four VWD sequences from vertebrate and invertebrate were aligned, and results have shown comparable similar regions from *E. sinensis* T20 to L36 (Fig. 2E). After mutating the T20/F21 (rΔVWD-1) and V35/L36 (rΔVWD-2) residues, the results have shown that rΔVWD-2 cannot affect rVWD inhibited bacterial growth, while rΔVWD-1 significantly affects rVWD inhibited bacterial growth (Fig. 2F), suggesting that T20/F21 amino acid residues that conserved between different species may have critical role on VWD inhibited bacterial growth.

EsVg enhances the phagocytosis of bacteria in hemocytes

EsVg-regulated phagocytosis has been confirmed in several other species, and the domains of EsVg have different bacteria-binding abilities (18, 19). Therefore, we investigated the ability of EsVg to reduce the number of bacteria via phagocytosis regulation. For this purpose, we precoated different strains of FITC-labeled bacteria with rEsVg-DUF1943 and rEsVg-VWD, which have shown bacterial binding activity.

In vivo phagocytosis assays demonstrated that rEsVg-DUF1943 strongly enhances the rate of *S. aureus* and *V. parahaemolyticus* phagocytosis by approximately 100% (Fig. 3), and rEsVg-VWD improves the rate of *S. aureus* and *V. parahaemolyticus* phagocytosis by approximately 70% (Fig. 3). Collective results indicated that bacterial interacted EsVg may enhance hemocytes phagocytosis via a phagocytic

in vivo, total hemocytes

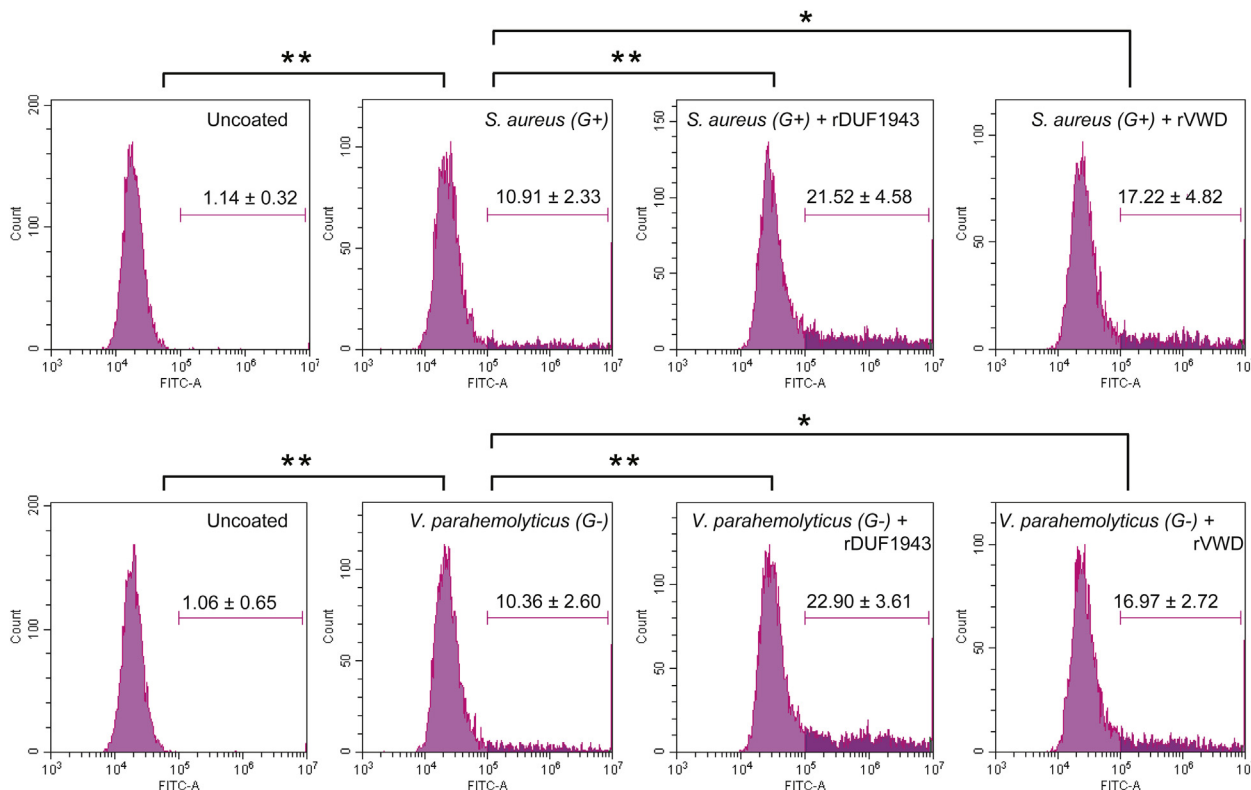


Figure 3. Promotion of hemocytic phagocytosis by EsVg. Different domains of EsVg promote phagocytosis of bacteria *in vivo*. *S. aureus* (Top panel) and *V. parahemolyticus* (Bottom panel) were heat-inactivated and labeled with FITC before coating with rDUF1943 and rVWD, respectively. The bacteria were then injected into the hemolymph and hemocytes were collected 1 h later for flow cytometric analysis. A total of 10,000 hemocytes were counted for each sample. Three independent repeats were performed, and results are expressed as the mean \pm SD. * $p < 0.05$, ** $p < 0.01$ (Student's *t* test).

receptor, which remain largely unexplored in both vertebrate and invertebrate.

cDNA cloning and bioinformatics analysis of EspIgr

The polymeric immunoglobulin receptor (pIgR) is an important component of the mucosal immune system. It mediates the transcytosis of polyimmunoglobulin (pIg) through epithelial cells to the mucosal surface to form Sigs, exerting immune defense functions in vertebrates (20, 21). However, information on pIgR in hemocyte endocytic processes remains limited. The possible relationship between Vg and pIgR has been reported in sea bass. Therefore, research on *E. sinensis* polymeric immunoglobulin receptor (EspIgr) is particularly important.

The 1662-bp open reading frame (ORF) region of EspIgr was cloned from the hemocytes of *E. sinensis*. The putative EspIgr protein contained 553 amino acids and an isoelectric point of 4.82, the ORF was predicted to encode a 60.7-kDa protein, and a signal peptide was located at their N terminus (Fig. 4A). Furthermore, three functional domains: an IG domain, two IG-like domains, and one transmembrane region were identified in the protein (Fig. 4, B–C). Phylogenetic analysis revealed three major branches that included vertebrates, crustacea, and insecta, with EspIgr clustered within the crustacea and close to insecta (Fig. 5).

Expression pattern of EspIgr

The EspIgr gene is expressed in different tissues harboring hemocytes (Fig. 6A), which indicates its role in crab immune regulation. To test whether EspIgr expression could be induced postinfection, *S. aureus* (Fig. 6B) and *V. parahemolyticus* (Fig. 6C) were used to infect crabs *in vivo*. Soon after infection with either pathogen, EspIgr expression is significantly induced, thus demonstrating its potential participation in innate immunity.

EsVg binding with EspIgr

EsVg may act as a potential receptor of EsVg on the hemocyte membrane. To elucidate whether binding might occur between EsVg and EspIgr and which domains of EsVg interact with EspIgr, the extracellular domain of EspIgr and three different domains of EsVg cDNA plasmids (LPD_N, DUF1943, VWD, and Δ DUF1943) were constructed and transfected into HEK293T cells (Fig. 7A). The coimmunoprecipitation results demonstrated that each plasmid was well expressed in these cells. Specifically, the EsVg-DUF1943 domain (FLAG-DUF) strongly binds with the EspIgr protein (HA-EspIgr). However, the EsVg-LPD_N domain (FLAG-LPD) and the EsVg-VWD domain (FLAG-VWD) did not bind with the EspIgr protein (Fig. 7B). Moreover, expressed plasmid that only contained LPD_N and VWD (Fig. 7C) cannot interaction with pIgR

Vitellogenin regulates phagocytosis in crab

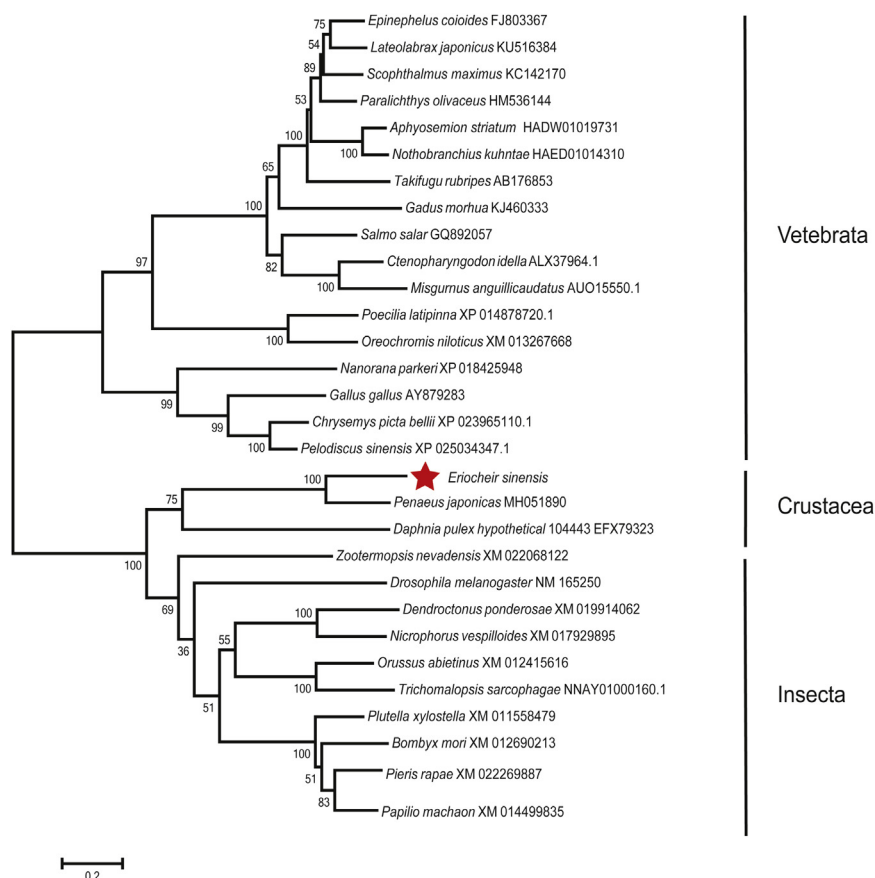


Figure 5. Neighbor-joining (NJ) phylogenetic analysis of EspIgR proteins. Phylogenetic analysis of EspIgR and some representative proteins from vertebrate and invertebrate species. The NJ phylogenetic tree was built in MEGA version 6 ($n = 1000$ bootstraps).

was added to crab hemocytes culture. Then, flow cytometry was performed to investigate the occurrence of hemocytic phagocytosis. The results show that, after stimulated with *S. aureus*, CPZ causes a dramatic decrease in hemocytic phagocytosis (Fig. 8B). The percentage of phagocytosis is $\sim 22.14\%$ in the *rEsVg*-DUF1943 group, which is higher than that in the CPZ and *rEsVg*-DUF1943 coinjection group ($\sim 8.97\%$). Similar results are also observed for the *V. parahaemolyticus* injection group (Fig. 8C). The percentage of phagocytosis is $\sim 21.50\%$ in the *rEsVg*-DUF1943 group, which is higher than that in the CPZ and *rEsVg*-DUF1943 coinjection group ($\sim 9.91\%$). Thus, these data indicate that the ability of *EsVg* to promote endocytosis is blocked by CPZ.

To confirm that the endocytosis of bacteria *via* the *EsVg*-EspIgR axis is clathrin-dependent, bacterial concentration in the primary-cultured crab hemocytes after being stimulated with *S. aureus* (Fig. 8F) and *V. parahaemolyticus* (Fig. 8G) was detected. The concentration of bacteria in the CPZ-added group is significantly higher than that in the controls. Thus, the results indicate that *EsVg*-EspIgR-mediated endocytosis is clathrin-dependent.

EsVg-EspIgR-mediated endocytosis protects the host from bacterial infection

To verify the role of *EsVg*-EspIgR-mediated endocytosis in innate immunity, two kinds of bacteria were coated with

rEsVg-DUF1943 in the presence or absence of siEspIgR and injected into crabs *in vivo*. Crab survival assay shown that *rEsVg*-DUF1943 significantly improved percent survival rate of crab post both *S. aureus* (Fig. 9A) and *V. parahaemolyticus* (Fig. 9B) infection in EspIgR-dependent manner. In coincidence, *rEsVg*-DUF1943 significantly suppressed hemocytes bacterial concentration in EspIgR-dependent manner post both *S. aureus* (Fig. 9C) and *V. parahaemolyticus* (Fig. 9D) infection. These results suggest that the *EsVg*-EspIgR axis plays critical roles in innate immunity by promoting hemocytic phagocytosis.

Discussion

Vg was initially regarded as a female-specific protein (24). However, Vg synthesis, albeit in small quantities, has been shown to occur in males and sexually immature animals, indicating that the function of Vg extends beyond that as an energy reserve for the nourishment of developing embryos (25). Previous studies on fish and mosquitos have demonstrated the crucial role of Vg on bacterial binding (6, 7), bacterial killing (19), and phagocytosis regulation profiles (6), but how Vg protein contributes to such diverse conserved immunological roles remains unknown. In the present study, we revealed that crab Vg binds bacteria *via* the DUF1943 and VWD domains and exerts antibacterial effects in a VWD-domain-dependent manner. Moreover, *EsVg* binds with

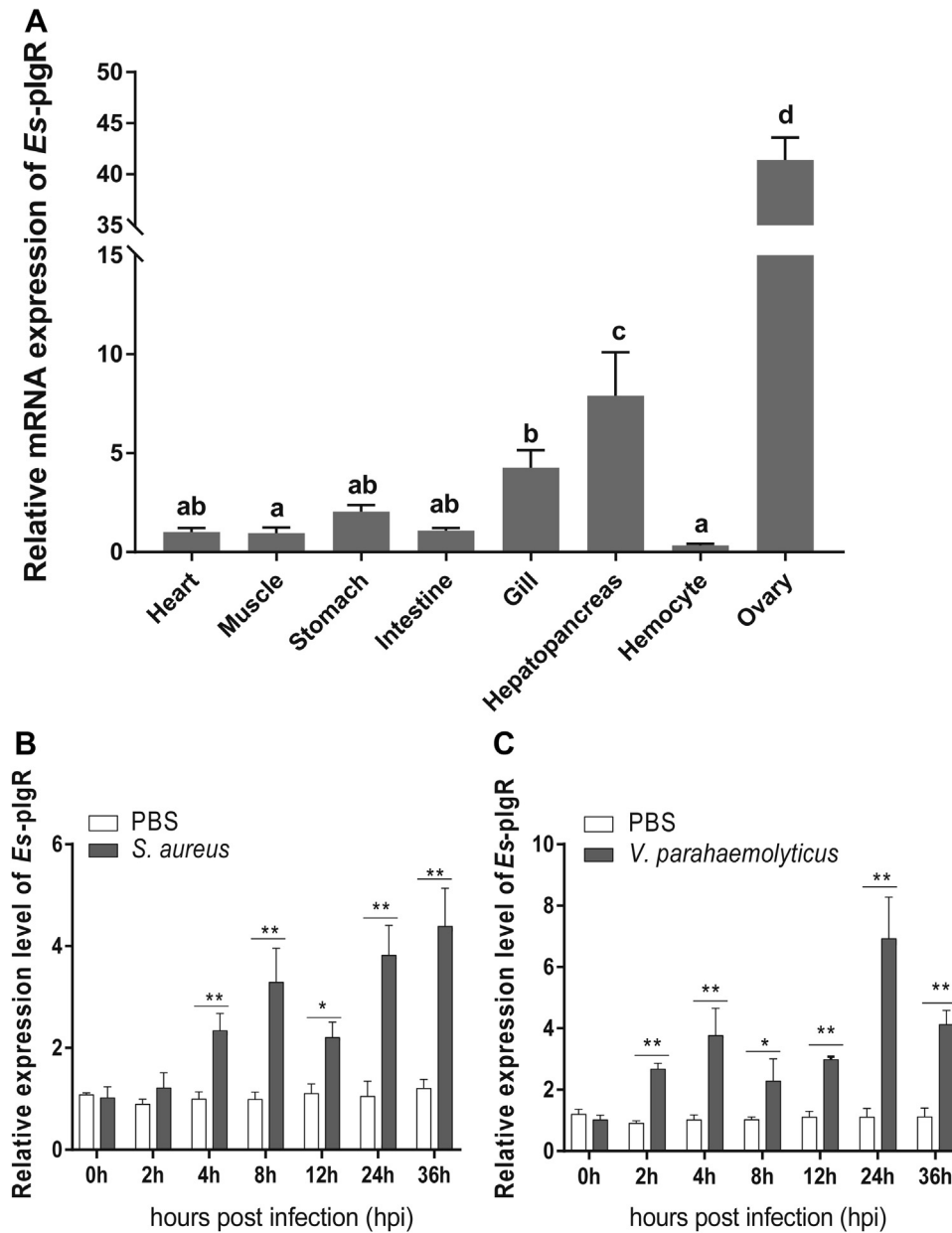


Figure 6. Expression pattern of EsplgR. A, tissue distribution of EsplgR. RNA samples were extracted from healthy *E. sinensis* crabs, and EsplgR expression was studied by RT-PCR (β -actin was the internal reference). Each sample was taken from at least three crabs, shown are the means \pm SD. Three independent repeats were performed (≥ 5 crabs per sample), with different lowercase indicated the significance (one-way ANOVA). B–C, expression profiles of EsplgR mRNA in crab hemocytes after infection by *S. aureus* (B) and *V. parahaemolyticus* (C). RNA was extracted at each time point. qRT-PCR was used to check the expression of EsplgR in each sample, with β -actin as the reference. Shown are the means \pm SD. Three independent repeats were performed (≥ 5 crabs per sample). * $p < 0.05$, ** $p < 0.01$ (Student's *t*-test).

EsplgR using the DUF1943 domain and promotes bacterial phagocytosis in hemocytes to control antibacterial functions. To the best of our knowledge, this study provides the first evidence for the critical role of different domains in EsVg in diverse antibacterial processes.

Vgs identified so far have been shown to share a similar domain structure combination. In most cases, Vgs include three conserved domains, *i.e.*, the LPD_N, DUF1943, and VWD domains (5). However, the functions of these domains in different species remain controversial. For instance, a study on zebrafish revealed that the DUF1943 and VWD domains

constitute a pattern-recognition system capable of interacting with bacteria and that DUF1943 functions as an opsonin capable of promoting the phagocytosis of bacteria by macrophages (13). Furthermore, a study on basal metazoan coral (*Euphyllia ancora*) revealed that all three domains in Vg not only interact with bacteria but also enhance phagocytosis (26). In the present study, we have shown that both DUF1943 and VWD domains bind with different bacterial strains *via* the signature components of LTA and LPS, which were similar with the results in zebrafish (13), suggesting the bacteria-binding function of these domains may be conserved across

Vitellogenin regulates phagocytosis in crab

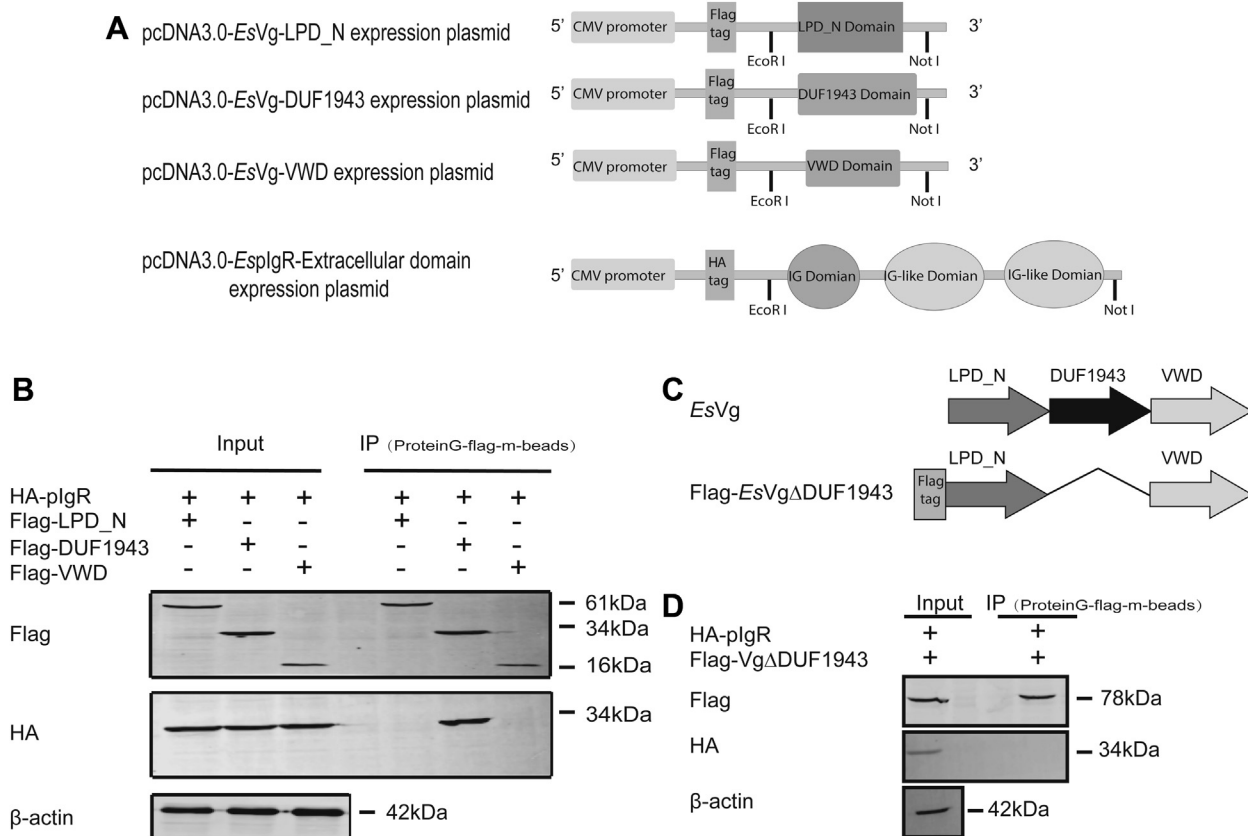


Figure 7. EsVg binding with EspIgR via DUF1943 domain. *A*, illustration of EspIgR and EsVg expression plasmids. *B*, coimmunoprecipitation assay results showing the interaction between different domains of EsVg proteins and EspIgR in HEK293T cells. Anti-FLAG and anti-HA antibodies were used to detect EsVg and EspIgR in coinfecting HEK293T cells, respectively. The anti-HA and anti-FLAG antibodies were incubated with the cell lysates and then isolated using Protein G-FLAG-m-beads. *C*, schematic diagram of Flag labeled truncated EsVg plasmid that without DUF1943 domain named Flag-EsVg Δ DUF1943. *D*, coimmunoprecipitation assay results showing undetected interaction between Flag-EsVg Δ DUF1943 and EspIgR in HEK293T cells. Anti-FLAG and anti-HA antibodies were used to detect EsVg and EspIgR in coinfecting HEK293T cells, respectively. Data are representative of at least three independent experiments.

vertebrates and invertebrates. Interestingly, only VWD domain exhibited strong bacteria growth inhibition activity. Although we did not test the antibacterial function of VWD in Vg of different species, the conserved amino acid residues mutated protein showed significantly lower bacteria growth inhibition activity, which indicated that antibacterial activity may act as a common signature for VWD from different species. Moreover, coimmunoprecipitation assay showed that only the DUF1943 domain binds with EspIgR, a crucial phagocytic receptor in arthropods, and strongly promotes hemocyte phagocytosis. However, it is still unclear whether the other two domains also regulate phagocytosis by different cell membrane receptors.

As a type I transmembrane glycoprotein, pIgR in different species shares four similar components: an intracellular region, a transmembrane region, a cleavage region, and an extracellular ligand-binding region (27). The Ig domains are located in the extracellular region (secretory component (SC)). Therefore, the N-terminal ligand-binding domain plays central roles in binding polymeric immunoglobulins. pIgR acts as a receptor for pIg and transports pIgA/pIgM across intestinal epithelial cells in vertebrates (28). In addition, pIgR and SC-mediated protection prevent the invasion of pathogenic microorganisms at mucosal surfaces (29, 30). Several studies on pIgR

found that certain microorganisms, such as *Streptococcus pneumoniae*, hijack pIgR to their own benefit during the invasion of host cells, indicating the crucial role of pIgR on endocytosis (31, 32). Recent studies on shrimp have indicated that pIgR is a WSSV receptor and that WSSV enters shrimp cells *via* the pIgR-CaM-Clathrin endocytosis pathway (22). Our results demonstrated that EspIgR is a phagocytic receptor for bacterial binding to EsVg, which highlights the important function of pIgR in crustacea and also indicates the multiple functions of pIgR in innate immunity.

In summary, three conserved domains, LPD_N, DUF1943, and VWD, were identified in crab Vg and found to facilitate diverse immunological functions. The DUF1943 and VWD domains bind with invading bacteria, and the VWD domain inhibits extracellular bacterial proliferation. Furthermore, the DUF1943 domain interacts with EspIgR at the cell membrane to promote hemocyte phagocytosis, thus ultimately fostering innate immunity in crabs (Fig. 9E).

Experimental procedures

Animals and primary-cultured hemocytes

Our experiments followed the protocol approved by the East China Normal University Animal Care and Use Committee

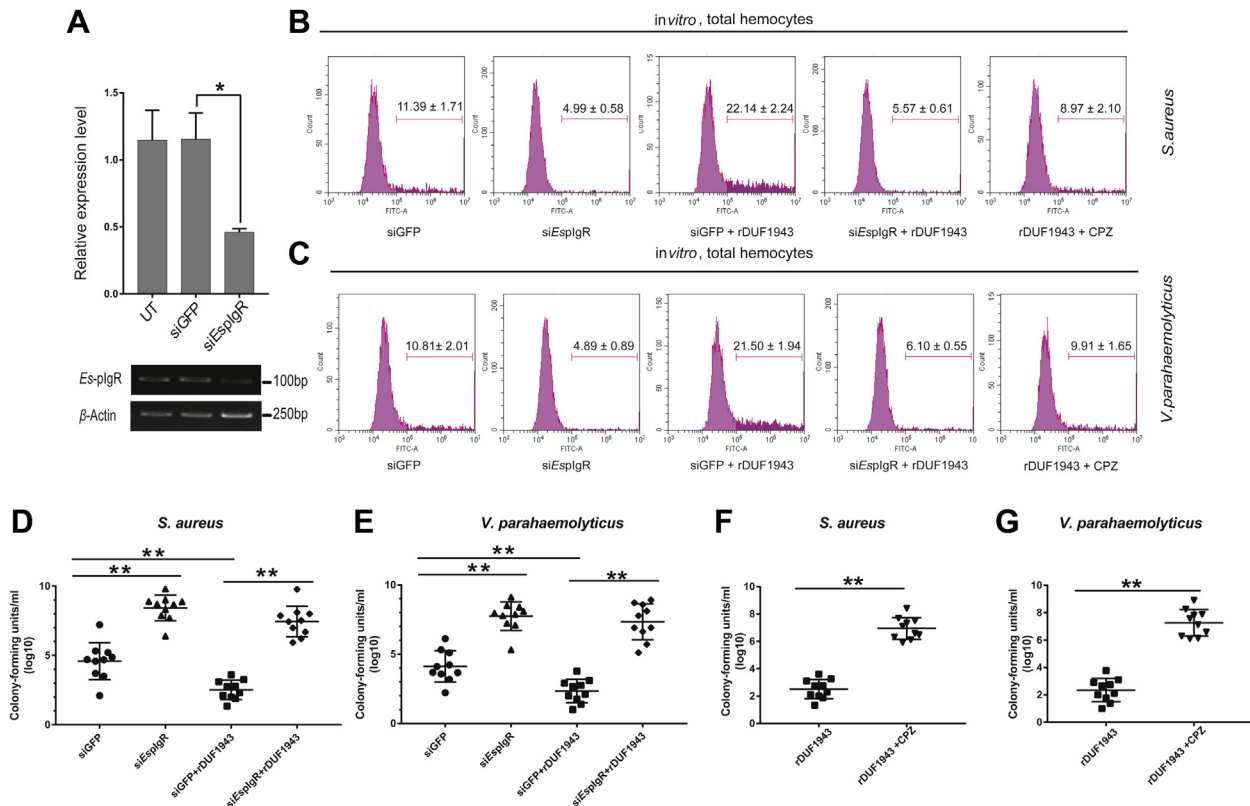


Figure 8. Bacteria enters hemocytes via EsVg-EsplgR-clathrin-mediated endocytosis. A, effects of RNAi on *EsplgR*. *EsplgR* siRNA (*siEsplgR*) was designed to knockdown *EsplgR* expression, and its expression in crab hemocytes was determined 24 h postinjection with *siEsplgR* by qRT-PCR (*siGFP* = control). Shown are means \pm SD from three independent repeats (≥ 3 crabs per sample). * $p < 0.05$ (Student's *t*-test). B–C, opsonin effect of the *EsVg-EsplgR* axis *in vitro*. *S. aureus* (B) and *V. parahaemolyticus* (C) were heat-killed, labeled with FITC, and fully coated with rDUF1943. The bacteria (1×10^6 CFU) were incubated with 1×10^6 hemocytes at 25 °C for 40 min. The mixture was centrifuged at 500g for 8 min to obtain the hemocytes. After washing, the hemocytes were analyzed by flow cytometry, where 10,000 hemocytes were counted for each sample. CPZ, an inhibitor of clathrin-mediated endocytosis, as well as rDUF1943-coated *S. aureus* (B) and *V. parahaemolyticus* (C) (1×10^8 CFU) were injected. Hemocytes were collected 40 min later and subjected to flow cytometry analysis. The phagocytosis ratios were calculated from three independent experiments, and the graphs are representative of the three repeats. D–E, RNAi of *EsplgR* or being fully coated by rDUF1943 affects bacterial proliferation in crab hemocyte medium supernatant. From each hemocytes medium, the supernatant was drawn at day 3 post-*S. aureus* (D) and post-*V. parahaemolyticus* (E) infection and plated onto agar plates for bacterial counting. F–G, injection of CPZ increases bacterial proliferation in crab hemocyte medium supernatant. The medium supernatant was drawn at day 3 post-*S. aureus* (F) and post-*V. parahaemolyticus* (G) infection and plated onto agar plates for bacterial counting.

(protocol license number AR2012/12017) in direct accordance with the Ministry of Science and Technology (China) for animal care guidelines. Healthy nonantibiotic or antifungal-fed *E. sinensis* crabs (100 ± 10 g each for adults and 20 ± 2 g each for naïve crabs) were obtained from the Songjiang aquatic farm (Shanghai, China). After quickly transferring them to the East China Normal University, all crabs were maintained in filtered and aerated freshwater provided with plenty of oxygen and fed daily with a commercial formulated diet containing no antibiotics.

Primary cultures of *E. sinensis* hemocytes were generated following established techniques (33). From the adult crabs, isolated hemocytes were gently resuspended in Leibovitz's L-15 medium (Sigma-Aldrich, Santa Clara, USA) supplemented with 1% antibiotics (10,000 U/ml penicillin, 10,000 μ g/ml streptomycin [Gibco, Waltham, USA]) and 0.2 mM NaCl (676 ± 5.22 mOsm/kg), at pH 7.20 to 7.40. Hemocytes were then counted with an automated cell counter (Invitrogen Countess, Waltham, USA) before seeding 4 ml (1×10^6 cells/ml) each into 60-mm dishes.

Immune stimulation and sample collection

S. aureus and *V. parahaemolyticus* were cultured, collected, and resuspended in sterile PBS (137 mM NaCl, 2.7 mM KCl, 10 mM Na_2HPO_4 , 2 mM KH_2PO_4 [pH 7.4]). Bacterial counts were determined by plating the diluted suspension onto agar plates.

For the *in vitro* bacterial stimulation, cultured *S. aureus* or *V. parahaemolyticus* (1×10^7 microbes per dish, 50 μ l) was added separately to the hemocyte-cultured dish, and sterile PBS (50 μ l) was used as the control. Total RNA was collected from hemocytes at specific times after stimulation. Three or more crabs were used per sample. First-strand cDNA was synthesized using a Reverse Transcriptase Kit (Takara, Osaka, Japan) following the manufacturer's instructions.

For the *in vivo* bacterial infection, *S. aureus* or *V. parahaemolyticus* (1×10^8 CFU per crab, 200 μ l) was injected into the hemolymph from the nonsclerotized membrane of the posterior walking leg, with sterile PBS (200 μ l) served as control. Total RNA was collected from hemocytes at specific time points after infection. At least three crabs were used per sample.

Vitellogenin regulates phagocytosis in crab

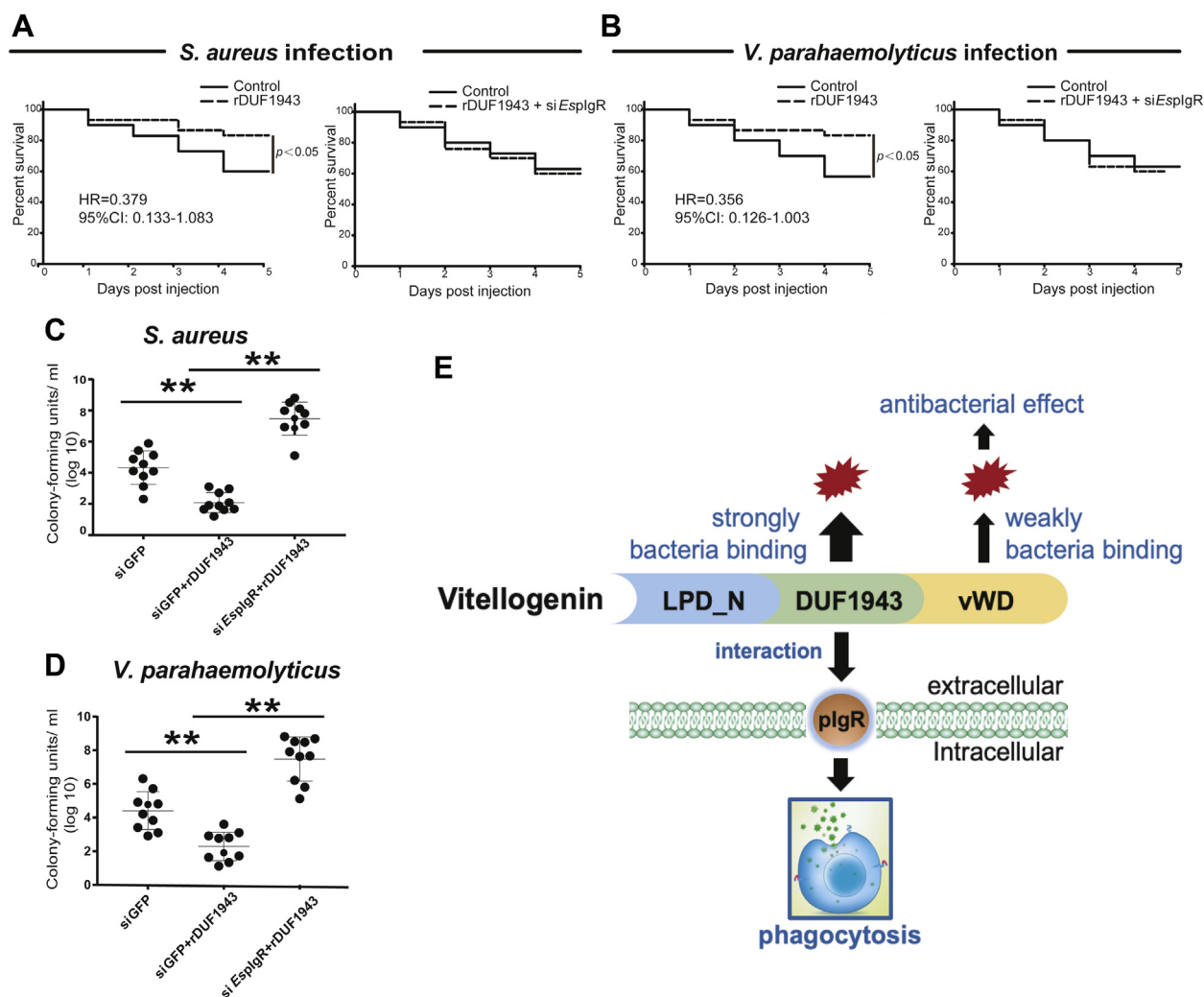


Figure 9. Protection of the crab host from bacterial infection via EsVg-EspIgr-mediated endocytosis. A–B, EsVg recombinant proteins improve crab survival while knockdown of EspIgr leads to crab death. Crabs were each injected with rDUF1943 and their 5-day survival post-*S. aureus* (A) and post-*V. parahaemolyticus* (B) infection was recorded from three independent repeats of 30 crabs per sample. In addition, survival rates with *S. aureus* (A) and *V. parahaemolyticus* (B) infection after being injected with siEspIgr and rDUF1943 were also recorded. Univariate Cox proportional hazards regression models were performed to estimate the crude hazard ratios (HRs) or adjusted HRs and their 95% confidential intervals (CIs). SPSS version 11.5 (SPSS Inc, Chicago, IL) software was used for analyses. C–D, recombinant protein of EsVg-DUF1943 reduces bacterial proliferation while RNAi of EspIgr increases bacterial proliferation in crabs treated as described above. From each crab, the hemolymph was drawn at day 3 post-*S. aureus* (C) and post-*V. parahaemolyticus* (D) infection and plated onto agar plates for bacterial counting. E, schematic of the EsVg-EspIgr axis promoting bacteria endocytosis. Shown are the means \pm SD. Three independent repeats were performed (≥ 5 crabs per sample). ** $p < 0.01$ (Student's *t*-test).

Genomic sequencing, assembly, annotation, and phylogenetic analysis

A fragment containing a full ORF encoding a protein with pIgr was identified from NCBI, and this was designated as EspIgr. Its full-length cDNA was amplified by a pair of gene-specific primers and then resequenced to confirm the accuracy. A similarity analysis was carried out using Clustalx from EMBL, with signal peptides and domain architecture predicted respectively by the SignalP v4.1 Server (<http://www.cbs.dtu.dk/services/SignalP/>) and SMART (<http://smart.embl-heidelberg.de/>), and protein 3D structure was predicted by the Swiss-PdbViewer (<https://spdbv.vital-it.ch/>). A phylogenetic tree was constructed based on the deduced amino acid sequences of EspIgr and other known pIgr by the neighbor-joining (NJ) algorithm using MEGA v6.0 software, bootstrap trials were replicated 1000 times.

RNA interference assay

cDNA fragments of EspIgr were PCR-amplified using primers linked to the T7 promoter (Table S1), to then serve as templates for producing siRNA with an *in vitro* T7 Transcription Kit (Fermentas, Burlington, Canada), with GFP siRNA purchased from the GenePharma Company (Shanghai, China) as the control. For the *in vitro* RNAi, the siRNA was dissolved in RNase-free water and transfected into *E. sinensis* primary-cultured hemocytes by using Lipofectamine 3000 (Thermo Fisher, Waltham, USA) to a final concentration of 10-nM. For the *in vivo* RNAi, the siRNA (1 μ g/g) was injected into the crab hemolymph. To extend the RNAi effect for crab survival assay, a second injection was administered to each crab at 2 days after the first-round injection. To determine RNAi efficiency, real-time RT-PCR was used with siGFP RNA as the control. After confirming the efficiency of RNAi assay,

S. aureus or *V. parahaemolyticus* was used to stimulate gene-silenced hemocytes *in vitro* or injected into gene-silenced crabs *in vivo*.

Gene expression profile analysis

Expression levels of *EspIgR* in the differently treated hemocytes were determined with quantitative RT-PCR (qRT-PCR; primers shown in Table S1) using a QuantStudio 5 Real-Time System (Applied Biosystems, USA) and SYBR Premix Ex Taq (Tli RNaseH Plus; TaKaRa, Osaka, Japan). Reaction conditions were used as following: 94 °C for 3 min, then 40 cycles at 94 °C for 10 s and 60 °C for 1 min, followed by melting from 65 to 95 °C. The gene expression levels were derived by the $2^{-\Delta\Delta CT}$ calculation method and normalized to the control group. Three independent experiments were performed and the results are presented as mean \pm SD

Expression and purification of recombinant protein

The recombinant expression plasmids pET-28a-LPD_N, pET-28a-DUF1943, and pET-28a-VWD were transformed into *E. coli* Transetta (DE3) (TransGen, Beijing, China). Single colonies of transformants were chosen and cultured to the mid-log phase (OD600 = 0.6). For expression of recombinant protein, four conditions were tested: 0.25 mM isopropyl b-D-1-thiogalactopyranoside (IPTG) for 3 h at 30 or 37 °C, and 1 mM IPTG for 3 h at 30 or 37 °C. The lysate of the induced cells was then collected after sonication and analyzed by 12% SDS-PAGE. Subsequently, the lysates were resuspended in binding buffer and the desired fusion protein purified using a Ni-NTA HisTrap FF crude column and washed with imidazole elution buffer (50 mM Tris-HCl, 300 mM NaCl, PH 7.5 and 250 mM imidazole) at 1 ml/min.

Assessment of crab survival and bacterial clearance assay

Crabs were randomly divided into eight groups each with 30 animals. After pretreating the crab with recombinant DUF1943 protein (rDUF1943), rDUF1943 plus *EspIgR* siRNA, or GFP siRNA, all crabs were injected with *S. aureus* or *V. parahaemolyticus* (1×10^9 CFU per crab, 200 μ l). Dead crabs in each group were counted daily, and survival was tabulated over 5 days. Three days after the bacterial injections, each crab's hemolymph was collected, diluted, and cultured overnight on solid LB plates, then bacterial colonies per plate were counted.

Microorganism-binding activity assay

Gram-positive bacteria (*S. aureus* and *Bacillus subtilis*) and Gram-negative bacteria (*Aeromonas hydrophila*, *V. parahaemolyticus*, *Vibrio anguillarum*, and *Edwardsiella tarda*) were cultured overnight in Luria–Bertani (LB) medium. The microorganisms were collected by centrifugation at 6000g and resuspended in 2 ml $1 \times$ TBS (Beyotime, China). Then, the microorganisms (2×10^7 CFU/ml in 500 ml of TBS) were incubated with 150 mg different purified Vg domain proteins for 1 h at 37 °C. After 6000g centrifugation for 5 min, the microorganisms were collected once again, washed three times with TBS, and finally resuspended in TBS. SDS-PAGE loading

buffer was added to each sample and then boiled for 8 min. The microorganism-binding activity of different *EsVg* domains was measured by western blotting with antiHis-tag mouse antibody (Beyotime, China).

LTA and LPS binding activity assay

Assay for binding of rDUF1943 and rVWD to LTA and LPS was conducted as previously described (13). Briefly, 100 μ l LTA (100 μ g/ml), LPS (100 μ g/ml), or PBS (pH 7.4) was mixed with 10 μ g of rDUF1943 or rVWD, respectively, and incubated for 1 h at 25 °C. After that, *S. aureus* cells (1×10^7 cells) were introduced in the LTA and PBS groups, and *V. parahaemolyticus* cells (1×10^7 cells) in the LPS and PBS groups. Bacterial cells were collected by incubation and centrifugation and the bacterial pellets were resuspended in 100 μ l of PBS. Subsequently, 10 μ l of each bacterial sample was electro-phoresed on a 12% SDS-PAGE gel and immunostained.

To quantify the binding of rDUF1943 and rVWD to LTA and LPS, ELISA was performed as described before (13). Briefly, the recombinant proteins were individually diluted in water to a concentration of 1 μ M. Fifty microliter of rDUF1943, rVWD, or TRX-His-tag peptide was applied to each well of a 96-well microplate and air-dried overnight at 20 °C. The plates were incubated at 60 °C for 30 min and blocked with 100 μ l of 1 mg/ml BSA in PBS at 37 °C for 2 h. After washing four times with PBST, biotin-labeled LTA or LPS was added into each well and incubated at 25 °C for 3 h, washed five times with 200 μ l of PBST, and incubated with 100 μ l of streptavidin–HRP (TransGen Biotech, Beijing, China) with 0.1 mg/ml BSA in PBS for 1 h. The wells were then washed and added with 75 μ l of 0.4 mg/ml O-phenylenedi-amine (Amresco) in the buffer and reacted at 37 °C for 10 min. Subsequently, H₂SO₄ (25 μ l of 2 M) was added into each well to terminate the reaction, and OD492 was monitored by a microplate reader (Bio-Rad, USA).

Antimicrobial activity assays

Growth curves of *S. aureus*, *V. parahaemolyticus*, *M. luteus*, and *E. coli* that cultured with recombinant LPD_N, DUF1943, VWD, or mutated VWD protein were detected according to the method that described previously (34). Site-directed mutagenesis was performed with Quik-Change kit (Stratagene) using primers listed in Table S1, and the mutation efficiency was confirmed by sequencing three individual clones from plasmids. The bacteria were cultured in the broth (LB and YPD, respectively) overnight until the OD600 reached about 0.8 to 1.0. After overnight culture, the purified recombinant protein was added to a final concentration of 20 mg/ml or 150 mg/ml, with Tris-buffered saline (TBS) as a control. The samples were incubated at 37 °C and centrifuged at 180 rpm, then the OD600 was measured every 2 h.

Coimmunoprecipitation

To confirm the interaction between *EsVg* and *EspIgR* *in vivo*, HEK293T cells were cultured for coimmunoprecipitation assays following previously reported methods (35).

Vitellogenin regulates phagocytosis in crab

Briefly, HEK293T cells were first seeded in 24-well plates and then cultured overnight in 37 °C DMEM (Life Technologies/Invitrogen, Carlsbad, CA) supplemented with 10% FBS (HyClone, Logan, UT) and 1% antibiotic-antimycotic solution (Life Technologies). After 24 h, cells were cotransfected with different Flag-tagged *EsVg* domain plasmids (pcDNA3.0-*EsVg*-LPD_N, pcDNA3.0-*EsVg*-DUF1943, pcDNA3.0-*EsVg*-VWD, and pcDNA3.0-*EsVg*- Δ DUF1943) and the HA-tagged extracellular domain of *EspIgR* (pcDNA3.0-*EspIgR*-extracellular domain), respectively, using Lipofectamine 3000 transfection reagent (Thermo Fisher, Waltham, USA) according to the manufacturer's instructions. At 36 h posttransfection, the HEK293T cells were washed twice with PBS before their proteins were extracted with an RIPA buffer, followed by centrifugation at 14,000g for 10 min. The supernatant was then precleared with 30 μ l of Protein A beads for 40 min at 4 °C with shaking and centrifuged at 12,000g for 10 min to remove the beads. The ensuing supernatant was incubated with 10 μ g of Flag and HA antibodies overnight at 4 °C under gentle rotation, added with Protein A beads, and incubated at 4 °C for 1 h to capture the antibodies. The centrifugation and PBS washing were employed to collect the beads, then resuspended in the SDS-PAGE loading buffer for separation by SDS-PAGE and western blot assays (using the Flag or HA antibody). All images were collected using an Odyssey CLx (LI-COR, Lincoln, USA).

Fluorescent labeling of bacteria and phagocytosis assay

Overnight-cultured *S. aureus* and *V. parahaemolyticus* were heat-killed and fluorescein isothiocyanate (Sigma, USA) conjugated. The bacterial suspension (1×10^8 microbes per milliliter, 1 ml) in PBS was mixed and incubated with 500 μ g of recombinant proteins by gentle rotation for 1 h at 28 °C to ensure full coating. The bacteria were pelleted and washed three times with PBS by centrifugation.

For the *in vitro* analysis, overnight cultures of bacteria were heat-inactivated at 72 °C for 20 min and collected by centrifugation, then cultured hemocytes (1×10^6 cells) were stimulated first with heat-killed bacteria (1×10^7 CFU) for 12 h and washed with PBS twice before the addition of approximately 1×10^6 (40 μ l) FITC-conjugated microbes coated with recombinant proteins. They were then incubated for 40 min at room temperature. For the *in vivo* analysis, the bacterial suspension (100 μ l) was injected into the hemolymph of crab at one of the posterior walking legs. One hour later, the hemocytes (6×10^5 cells) were isolated from the other of the posterior walking legs and centrifuged at 300g for 10 min at 4 °C and washed with PBS three times. After that, the phagocytosis rate in 1 ml of each sample was determined by flow cytometry using a CytoFLEX apparatus (Beckman, USA), and the data were analyzed using CytExpert software. At least 10,000 hemocytes taken from three crabs were counted for each sample. The experiments were repeated three times. Three days after the bacterial injections, each crab's hemolymph or medium supernatant was drawn, diluted, and cultured overnight on solid LB plates, then bacterial colonies per plate were counted.

Chlorpromazine injection

To detect the endocytosis of bacteria, the clathrin-dependent endocytosis inhibitor chlorpromazine (CPZ, Sangon Biotech, Shanghai, China) and 500 μ g of recombinant proteins fully coated with bacteria (1×10^8 CFU) were added to primary-cultured crab hemocytes medium according to previous described method (22). The phagocytosis rate in 1 ml of each sample was determined by flow cytometry using a CytoFLEX apparatus (Beckman, USA), and the data were analyzed using CytExpert software. The resulting plots are representative of three independent assays, and the phagocytosis ratios were calculated from those three tests.

Data availability

All data are contained within the article.

Acknowledgments—We thank the Experimental Platform for Molecular Zoology (East China Normal University, Shanghai, China) for providing instruments essential for conducting this study.

Author contributions—W. K. S. data curation; W. K. S and H. L. formal analysis; Q. W. and W. W. L. funding acquisition; W. K. S., Q. W., and W. W. L. validation; W. K. S., H. L., Y. H. Z., and L. W. B. investigation; Y. K. Q. and W. W. L. visualization; W. K. S. and W. W. L. writing-original draft; W. W. L. writing-review and editing; Q. W. and W. W. L. conceptualization; Q. W. and W. W. L. supervision; W. W. L. project administration.

Funding and additional information—This work was supported by National Natural Science Foundation of China (31672639 and 31970490 to Q. W., 31972820 to W. L.) and Shanghai Rising-Star Program (20QA1403000 to W. L.).

Conflict of interest—The authors declare that they have no conflicts of interest with the contents of this article.

Abbreviations—The abbreviations used are: CPZ, chlorpromazine; *EspIgR*, *E. sinensis* polymeric immunoglobulin receptor; IPTG, isopropyl b-D-1-thiogalactopyranoside; LB, Luria-Bertani; LLTP, large lipid transfer protein; NJ, neighbor-joining; ORF, open reading frame; pIg, polyimmunoglobulin; pIgR, polymeric immunoglobulin receptor; SC, secretory component; TBS, Tris-buffered saline; Vg, vitellogenin; VWD, von Willebrand factor type D domain.

References

1. Avarre, J. C., Lubzens, E., and Babin, P. J. (2007) Apolipoprotein, formerly vitellogenin, is the major egg yolk precursor protein in decapod crustaceans and is homologous to insect apolipoprotein II/I and vertebrate apolipoprotein B. *BMC Evol. Biol.* 7, 3
2. Babin, P. J., and Gibbons, G. F. (2009) The evolution of plasma cholesterol: direct utility or a "spandrel" of hepatic lipid metabolism? *Prog. Lipid Res.* 48, 73–91
3. Arukwe, A., and Goksøyr, A. (2003) Eggshell and egg yolk proteins in fish: hepatic proteins for the next generation: oogenetic, population, and evolutionary implications of endocrine disruption. *Comp. Hepatol.* 2, 4
4. Li, H., and Zhang, S. (2017) Functions of vitellogenin in eggs. *Results Probl. Cell Differ.* 63, 389–401
5. Zhang, S., Wang, S., Li, H., and Li, L. (2011) Vitellogenin, a multivalent sensor and an antimicrobial effector. *Int. J. Biochem. Cell Biol.* 43, 303–305

6. Li, Z., Zhang, S., and Liu, Q. (2008) Vitellogenin functions as a multi-valent pattern recognition receptor with an opsonic activity. *PLoS One* **3**, e1940
7. Li, Z., Zhang, S., Zhang, J., Liu, M., and Liu, Z. (2009) Vitellogenin is a cidal factor capable of killing bacteria via interaction with lipopolysaccharide and lipoteichoic acid. *Mol. Immunol.* **46**, 3232–3239
8. Garcia, J., Munro, E. S., Monte, M. M., Fourrier, M. C., Whitelaw, J., Smail, D. A., and Ellis, A. E. (2010) Atlantic salmon (*Salmo salar* L.) serum vitellogenin neutralises infectivity of infectious pancreatic necrosis virus (IPNV). *Fish Shellfish Immunol.* **29**, 293–297
9. Rono, M. K., Whitten, M. M., Oulad-Abdelghani, M., Levashina, E. A., and Marois, E. (2010) The major yolk protein vitellogenin interferes with the anti-plasmodium response in the malaria mosquito *Anopheles gambiae*. *PLoS Biol.* **8**, e1000434
10. Huo, Y., Yu, Y., Chen, L., Li, Q., Zhang, M., Song, Z., Chen, X., Fang, R., and Zhang, L. (2018) Insect tissue-specific vitellogenin facilitates transmission of plant virus. *PLoS Pathog.* **14**, e1006909
11. Salmela, H., Amdam, G. V., and Freitag, D. (2015) Transfer of immunity from mother to offspring is mediated via egg-yolk protein vitellogenin. *PLoS Pathog.* **11**, e1005015
12. Tufail, M., and Takeda, M. (2008) Molecular characteristics of insect vitellogenins. *J. Insect Physiol.* **54**, 1447–1458
13. Sun, C., Hu, L., Liu, S., Gao, Z., and Zhang, S. (2013) Functional analysis of domain of unknown function (DUF) 1943, DUF1944 and von Willebrand factor type D domain (VWD) in vitellogenin2 in zebrafish. *Dev. Comp. Immunol.* **41**, 469–476
14. Ibanez, F., Tang, X., and Tamborindeguy, C. (2018) Bactericera cockerelli vitellogenin-6 like, a vitellogenin without a direct reproductive function? *Insect Mol. Biol.* **27**, 166–176
15. Park, H. G., Lee, K. S., Kim, B. Y., Yoon, H. J., Choi, Y. S., Lee, K. Y., Wan, H., Li, J., and Jin, B. R. (2018) Honeybee (*Apis cerana*) vitellogenin acts as an antimicrobial and antioxidant agent in the body and venom. *Dev. Comp. Immunol.* **85**, 51–60
16. Singh, J., and Aballay, A. (2017) Endoplasmic reticulum stress caused by lipoprotein accumulation suppresses immunity against bacterial pathogens and contributes to immunosenescence. *mBio* **8**, e00778-17
17. Tong, Z., Li, L., Pawar, R., and Zhang, S. (2010) Vitellogenin is an acute phase protein with bacterial-binding and inhibiting activities. *Immunobiology* **215**, 898–902
18. Hystad, E. M., Salmela, H., Amdam, G. V., and Münch, D. (2017) Hemocyte-mediated phagocytosis differs between honey bee (*Apis mellifera*) worker castes. *PLoS One* **12**, e0184108
19. Liu, M., Pan, J., Ji, H., Zhao, B., and Zhang, S. (2011) Vitellogenin mediates phagocytosis through interaction with FcγR. *Mol. Immunol.* **49**, 211–218
20. Mostov, K. E. (1994) Transepithelial transport of immunoglobulins. *Annu. Rev. Immunol.* **12**, 63–84
21. Turula, H., and Wobus, C. E. (2018) The role of the polymeric immunoglobulin receptor and secretory immunoglobulins during mucosal infection and immunity. *Viruses* **10**, 237
22. Niu, G. J., Wang, S., Xu, J. D., Yang, M. C., Sun, J. J., He, Z. H., Zhao, X. F., and Wang, J. X. (2019) The polymeric immunoglobulin receptor-like protein from *Marsupenaeus japonicus* is a receptor for white spot syndrome virus infection. *PLoS Pathog.* **15**, e1007558
23. Yang, S., Liu, S., Qu, B., Dong, Y., and Zhang, S. (2017) Identification of sea bass pIgR shows its interaction with vitellogenin inducing antibody-like activities in HEK 293T cells. *Fish Shellfish Immunol.* **63**, 394–404
24. Pan, M. L., Bell, W. J., and Telfer, W. H. (1969) Vitellogenic blood protein synthesis by insect fat body. *Science* **165**, 393–394
25. Piulachs, M. D., Guidugli, K. R., Barchuk, A. R., Cruz, J., Simões, Z. L., and Bellés, X. (2003) The vitellogenin of the honey bee, *Apis mellifera*: structural analysis of the cDNA and expression studies. *Insect Biochem. Mol. Biol.* **33**, 459–465
26. Du, X., Wang, X., Wang, S., Zhou, Y., Zhang, Y., and Zhang, S. (2017) Functional characterization of Vitellogenin_N domain, domain of unknown function 1943, and von Willebrand factor type D domain in vitellogenin of the non-bilaterian coral *Euphyllia ancora*: implications for emergence of immune activity of vitellogenin in basal metazoan. *Dev. Comp. Immunol.* **67**, 485–494
27. Kaetzel, C. S. (2005) The polymeric immunoglobulin receptor: bridging innate and adaptive immune responses at mucosal surfaces. *Immunol. Rev.* **206**, 83–99
28. Hamuro, K., Suetake, H., Saha, N. R., Kikuchi, K., and Suzuki, Y. (2007) A teleost polymeric Ig receptor exhibiting two Ig-like domains transports tetrameric IgM into the skin. *J. Immunol.* **178**, 5682–5689
29. Phalipon, A., Cardona, A., Kraehenbuhl, J. P., Edelman, L., Sansonetti, P. J., and Corthésy, B. (2002) Secretory component: a new role in secretory IgA-mediated immune exclusion *in vivo*. *Immunity* **17**, 107–115
30. Robinson, J. K., Blanchard, T. G., Levine, A. D., Emancipator, S. N., and Lamm, M. E. (2001) A mucosal IgA-mediated excretory immune system *in vivo*. *J. Immunol.* **166**, 3688–3692
31. Kaetzel, C. S. (2001) Polymeric Ig receptor: defender of the fort or Trojan horse? *Curr. Biol.* **11**, R35–R38
32. Zhang, J. R., Mostov, K. E., Lamm, M. E., Nanno, M., Shimida, S., Ohwaki, M., and Tuomanen, E. (2000) The polymeric immunoglobulin receptor translocates pneumococci across human nasopharyngeal epithelial cells. *Cell* **102**, 827–837
33. Yang, L., Li, X., Qin, X., Wang, Q., Zhou, K., Li, H., Zhang, X., Wang, Q., and Li, W. (2019) Deleted in azoospermia-associated protein 2 regulates innate immunity by stimulating Hippo signaling in crab. *J. Biol. Chem.* **294**, 14704–14716
34. Li, L., Li, X. J., Wu, Y. M., Yang, L., Li, W., and Wang, Q. (2017) Vitellogenin regulates antimicrobial responses in Chinese mitten crab, *Eriocheir sinensis*. *Fish Shellfish Immunol.* **69**, 6–14
35. Li, D., Wan, Z., Li, X., Duan, M., Yang, L., Ruan, Z., Wang, Q., and Li, W. (2019) Alternatively spliced down syndrome cell adhesion molecule (Dscam) controls innate immunity in crab. *J. Biol. Chem.* **294**, 16440–16450